Jül-Conf-45 D1-3

I C A N S - V
MEETING OF THE INTERNATIONAL COLLABORATION ON
ADVANCED NEUTRON SOURCES
June 22-26, 1981

Differential Production Cross Sections for Charged Particles Produced by 590 MeV Proton Bombardment of Thin Metal Targets

S.D. HOWE, S. CIERJACKS, Y. HINO, F. RAUPP, M.T. RAINBOW, M.T. SWINHOE, AND L. BUTH.

KERNFORSCHUNGSZENTRUM KARLSRUHE
INSTITUT FÜR KERNPHYSIK
7500 KARLSRUHE, POSTFACH 3640
FEDERAL REPUBLIC OF GERMANY

Abstract

Differential production cross sections have been measured for the reactions (p,p), (p,d), (p,t) and (p,π±) using the 590 MeV proton beam at SIN. Here we report measurements made on thin targets of aluminium, niobium, lead, and uranium at laboratory angles of 90^{o} and 157^{o}. The data were taken over a proton energy range of about 50 MeV to 590 MeV. Differential cross sections are reported along with predictions by the intranuclear-cascade/evaporation model as computed by HETC.

1. INTRODUCTION

The use of high-current, medium-energy particle accelerators as spallation sources for nuclear research has gained widespread interest in recent years. Along with fundamental research, work performed at such facilities can provide valuable information in accessing the feasibility of using large scale spallation sources to breed nuclear fuel for conventional nuclear reactors. Design of such facilities, however , depends heavily on the characterisation of the particle spectra emitted by spallation targets.

Several researchers [1-6] have investigated the differential and integral neutron yields leaking out of large spallation targets. Comparisons between such measurements and predicted values calculated by the intranuclear-cascade/evaporation model have revealed a wide range of disagreement. Comparison of differential neutron spectra form thin targets have shown good agreement with calculated values for the evaporation, $E < 20$ MeV, region of the spectrum. For energies greater than 20 MeV, however, discrepencies exist between calculation and measurement.

Consequently, we have performed a series of measurements to determine the differential leakage spectra of protons, deuterons, tritons, and charged pions from thin targets bombarded by 590 MeV protons. Results at laboratory angles of 90^{o} and 157^{o} for targets of aluminium, niobium, lead, and uranium are reported.

2. EXPERIMENT

The measurements were performed using the 590 MeV proton beam of the SIN cyclotron in Switzerland. Proton pulses at a frequency of 16.84 MHz were impinged on thin metal targets of Al, Nb, Pb and U with thickness of 0.86, 3.43, 4.99, and 5.92gm/cm^2 respectively. The incident proton number was monitored using a small scatterer with a scintillator telescope which was calibrated periodically during the measurements.

The experimental set-up is shown in Fig.1. A more detailed description is presented elsewhere.[7] In brief, our assembly consisted of a 4.50 cm diameter by 3 cm deep NE213 liquid scintillator, D_2, positioned at 90^{o} and then 157^{o} with respect to the incident proton beam axis. The detector provided timing, pulse height, and pulse-shape-discrimination information which was recorded in an event-by-event mode. A thin plastic scintillator placed halfway between D_2 and the target was used in a single coincidence mode to denote charged particles. Total time-of-flight paths were through air and were 4.23 m and 1.87 m for 90^{o} and 157^{o} respectively.

In order to reduce the random coincidence rate due to neutron events in the NE213 detector, we placed an open ended lead cave around and extending 30-40 cm in front of the detector. About 1 m of lead shielding was also used to seclude the beam monitor scatter from the target-detector area.

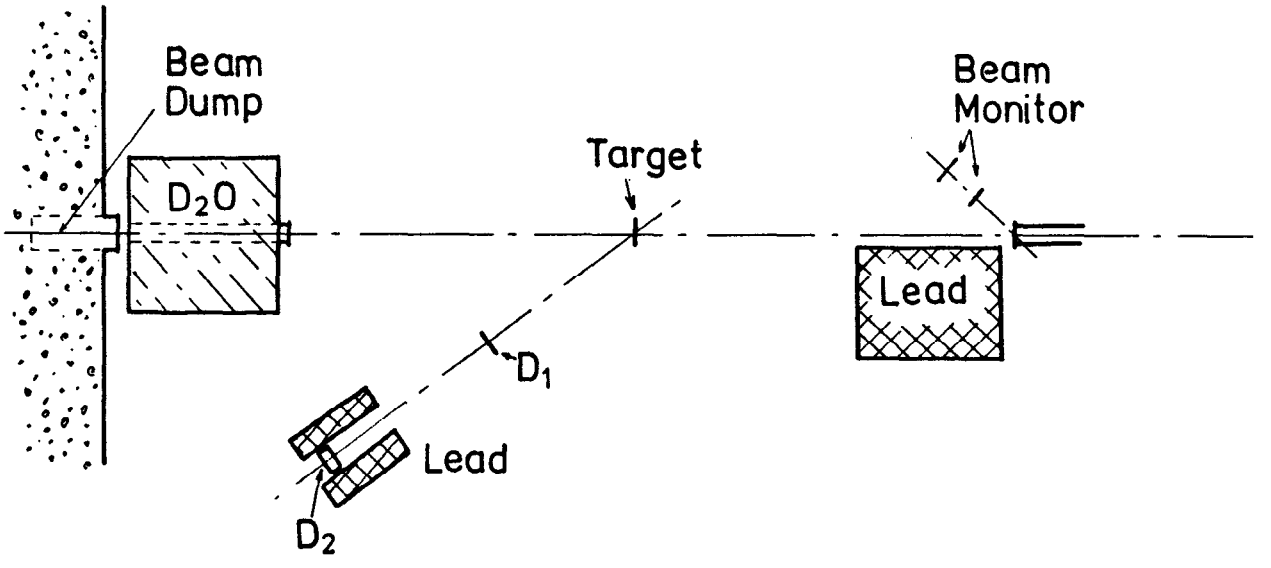

Figure 1: Experimental set-up for this measurement. D_1 and D_2 were a 0.2 cm thick plastic and a 3.0 cm thick Ne-213 scintillator respectively.

Results and Discussion

The results of these measurements are shown in Figs. 2 to 9 as differential cross sections as a funtion of the energy of the observed particle. In each case, the data have been corrected for energy losses of the secondary particle in the target material and intervening air path.

The results for secondary proton emission are shown in Figs. 2 and 3. The cross sections are seen to vary smoothly over the energy range considered up to maximum energies of about 360 MeV and 220 meV for 90^{o} and 157^{o} respectively. The data at 157^{o} are also seen to decrease more rapidly with increasing energy than those at 90^{o}. These effects and the reduction at 157^{o} relative to 90^{o} of the general magnitude of the cross sections are all indicative of the intranucleon cascade process which is strongly forward peaked.

Spectra for deuteron and triton production cross sections are shown in Figs. 4 to 7. The upper energy limit of the deuteron data is determined by the pulse-height resolution of our scintillation detector. For energies greater than those seen in Figs. 4 and 5, the separate proton-deuteron pulse-height peaks could no longer be resolved. Extrapolations of the deuteron data were subtracted from the proton results but are not reported with the deuteron values. Such corrections to the proton areas were typically $\leq$ 10%.

From the figures, we see that the deuteron values appear to follow an exponential behaviour as a function of particle energy. Performing least-square-fits to the data shows that the exponential coefficient is different for each angle but is relatively independent of the nucleon number in the target nucleus. Comparison of the fits at each angle shows that the slope of the data is much steeper for 157° than for 90° which is a result similar to the proton behaviour.

We can also observe an exponential behaviour for the triton emission results but the statistical errors of the data are greater and such behaviour is not entirely evident. Unlike the proton and deuteron results, though, the general trends of the cross sections appear to decrease at the same rate at both 90° an 157°. This may indicate that the heavier tritons are emitted later in the cascade process from a nuclens in a pre-equilibrium state.

The production cross sections of charged pions seen in Figs. 8 and 9 have a lower energy limit which is also determined by the inability to resolve separate proton and pion pulse height responses. The figures show that the cross sections are somewhat backward peaked and that the average energy in the backward direction is substantially smaller. The average energies were about 98 MeV and 63 MeV for 90° and 157° respectively and appear to be relatively independent of target nucleon number.

Integration of the differential spectra with respect to energy gives a good indication of the relative magnitudes of the cross sections for the different particles. In Table I, the integral values show that the production cross sections for protons, deuterons, and tritons are separated by about an order of magnitude. The results also show that the particle production at 157° relative to that at 90° is about a factor of 3.6, 5.3, 7.6, and 0.73 for protons, deuterons, tritons, and pions respectively.

TABLE I

Cross sections in mb/sr resulting from integration of the differential spectra over the observed energy range

	particle	Al	Nb	Pb	U
90^o	P	18.2	53.4	88.3	97.6
	d	.840	2.68	4.50	5.17
	T	.051	.190	.399	.438
	π	2.61	4.98	6.62	7.36
157^o	P	5.42	14.69	25.1	26.0
	d	.156	.462	.935	.988
	T	.0068	.0191	.0611	.0695
	π	3.16	6.60	10.4	10.5

Model Calculations

Calculations of charged particle production from thin targets of aluminum and lead have been performed using the HETC computer code[9]. Comparisons of the code's predictions for protons and pions at 90^o and 157^o are shown in Figs. 10 to 13. Comparisons of deuteron and triton results are not possible since the code only calculates deuteron and triton spectra emitted from the evaporation process. The calculations had an upper energy of about 30 MeV while the lower energy limit of our data was about 70 to 80 MeV.

In Figs. 10 and 11, we see that the calculations tend to underpredict our measured results for lead by about a factor of 2 throughout most of the energy range. At 90^o, however, the code overpredicts the results at the upper energies and, in general, predicts a slightly different spectrum shape. For aluminum, the predictions are about a factor of 0.6 below the experimental values at 90^o but are also a factor of 2 too low at 157^o. The underpredictions by the code may indicate that nucleon clustering in the nucleus during the cascade, which HETC does not take into account, might be significant.

The HETC predictions and experimental results for charged pion production are compared in Figs. 12 and 13. Also shown in Fig. 12 are results of another experiment which measured differential production cross sections of π^+ and π^- separately. In these figures, we see that the calculations overestimate the measured values rather drastically. Although the agreement is better at 157^o than at 90^o, the spectra are still separated by a factor of 2 to 3. Consequently,

we feel that the angular distributions used in the code for the pion production processes should be carefully reexamined.

5. CONCLUSION

In conclusion, we have determined the differential production cross sections of protons, deuterons, tritons and pions for 590 MeV proton bombardement of thin metal targets at laboratory angles of 90^{o} and 157^{o}. The proton data are seen to decrease smoothly with increasing particle energy until an energy maximum, of about 360 MeV and 220 MeV for protons at 90^{o} and 157^{o} respectively, is reached. At both angles, the deuterium cross sections appear to follow an exponential behaviour and are about an order of magnitude smaller than the proton values. Similar behaviour is seen in the triton spectra with still another factor of 10 reduction in magnitude. The triton spectra also appear to be produced by a nucleus in a pre-equilibrium state.

Comparison between our results and calculations by the HETC computer code show a significant underprediction of the proton values by the code and an overprediction of the pion results. The comparisons indicate that 1) the effect of nucleon clustering in the nucleus may be important during the cascade process, and 2) the angular distribution used in the code for the pion production mechanisms needs review. In the near future, we intend to supplement these results with data taken at 23^{o}, 45^{o}, and 135^{o} in order to develop a more complete understanding of behaviour of the spallation process.

The authors would like to acknowledge the help of the SIN staff, especially Dr. W. Fischer and Dr. C. Tschalär. We are also indebted to Dr. C. Weddigen and Dr. J. Hoftiezer for their advice and the loan of miscellaneous equipment.

REFERENCES

1. J.S. FRASER, et al., Physics in Canada 21, No. 2, 17018 (1965).
2. R. Madey and F.M. Waterman, Phys. Rev. C8, 2412 (1973).
3. C.G. Cassapakis, et al., Phys. Lett. 63B, 35 (1976).
4. G.J. Russell, et al., Intl. Conf. on Neutron Physics and Nucl. Data for Reactors and Other Appl. Purposes, Harwell, England (1978).
5. H. Takahashi and Y. Nakahara, Int. Conf. of Neut. Cross Sections for Technology, (1979).
6. P.M. Garvey, Proc. of Meeting on Targets for Neutron Beam Spallation Neutron Sources, Jül-Conf-34, ISSN 0344-5798, Jülich (1980).
7. S. Cierjacks, Proc. of ICANS-V Conf., Jülich (1981). (to be published)
8. J.F. Crawford, et. al., Phys. Rev. C, 22 , No. 3, 1184 (1980).
9. Filgess and T. Armstrong, Proc. of ICANS-V Conf, Jülich (1981)

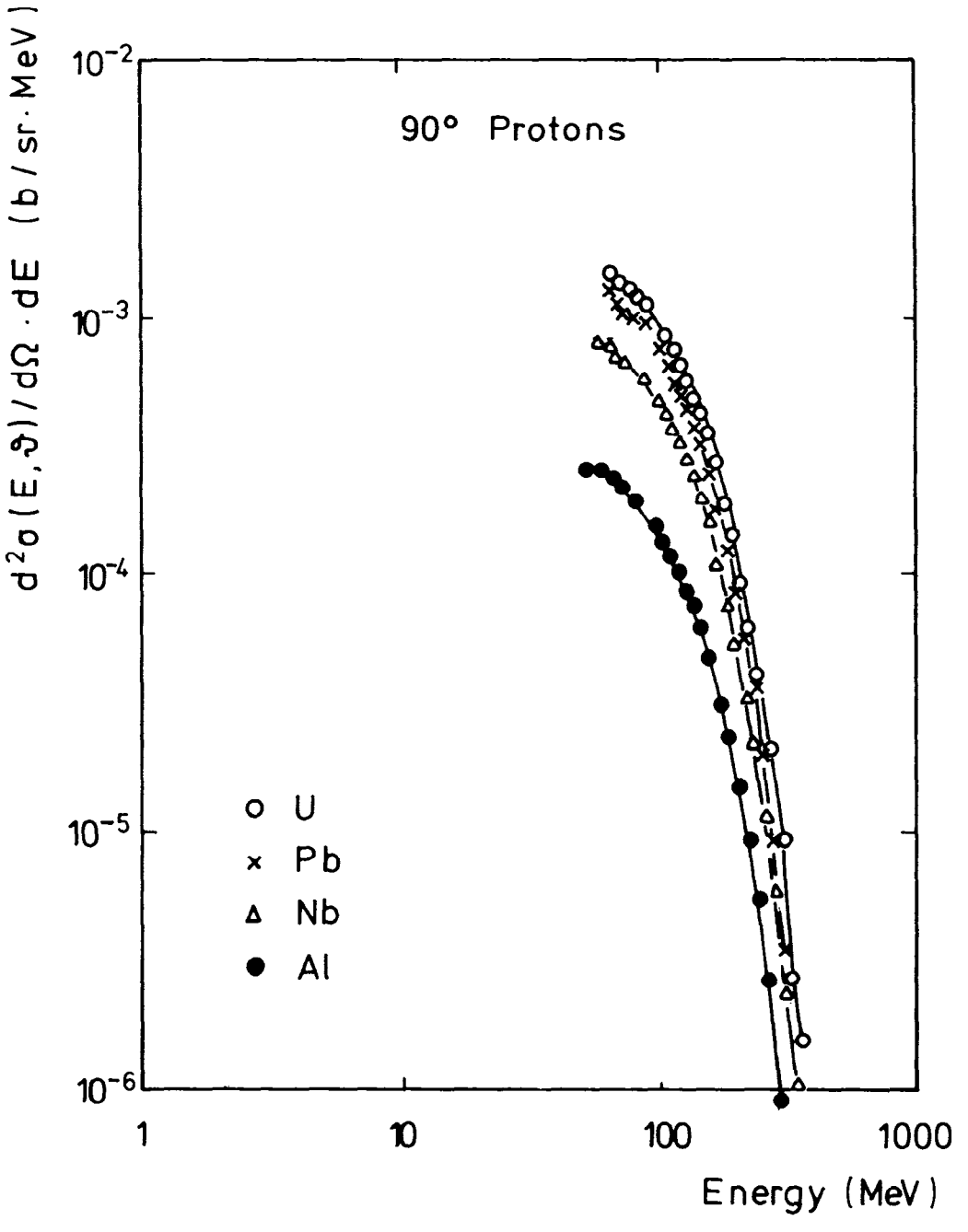

Figure 2 - Differential cross sections for secondary protons emitted from aluminum, niobium, lead, and uranium at a laboratory angle of 90°. The character size indicates the statistical uncertainty.

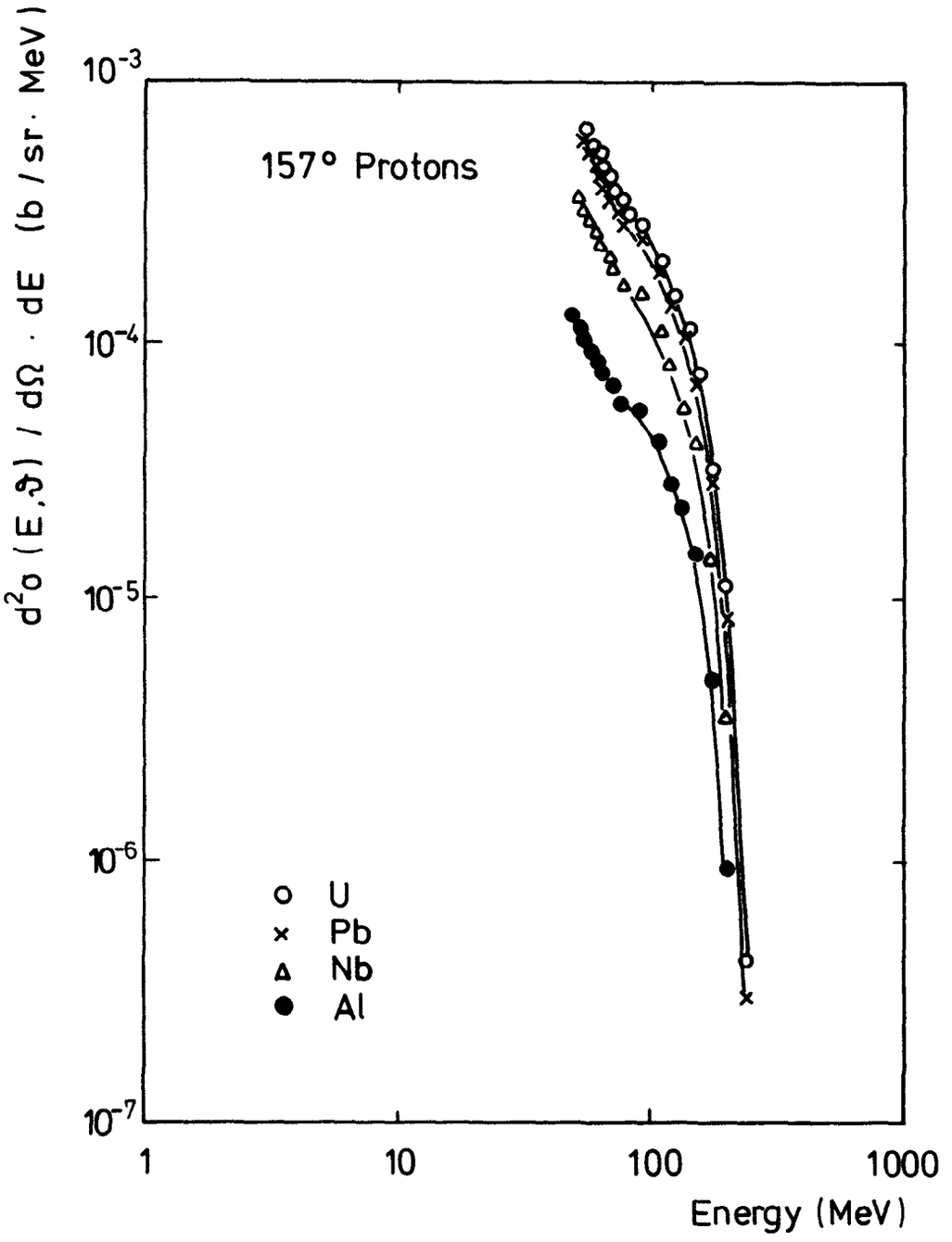

Figure 3 - Same as Fig. 2 except for a laboratory angle of 157°.

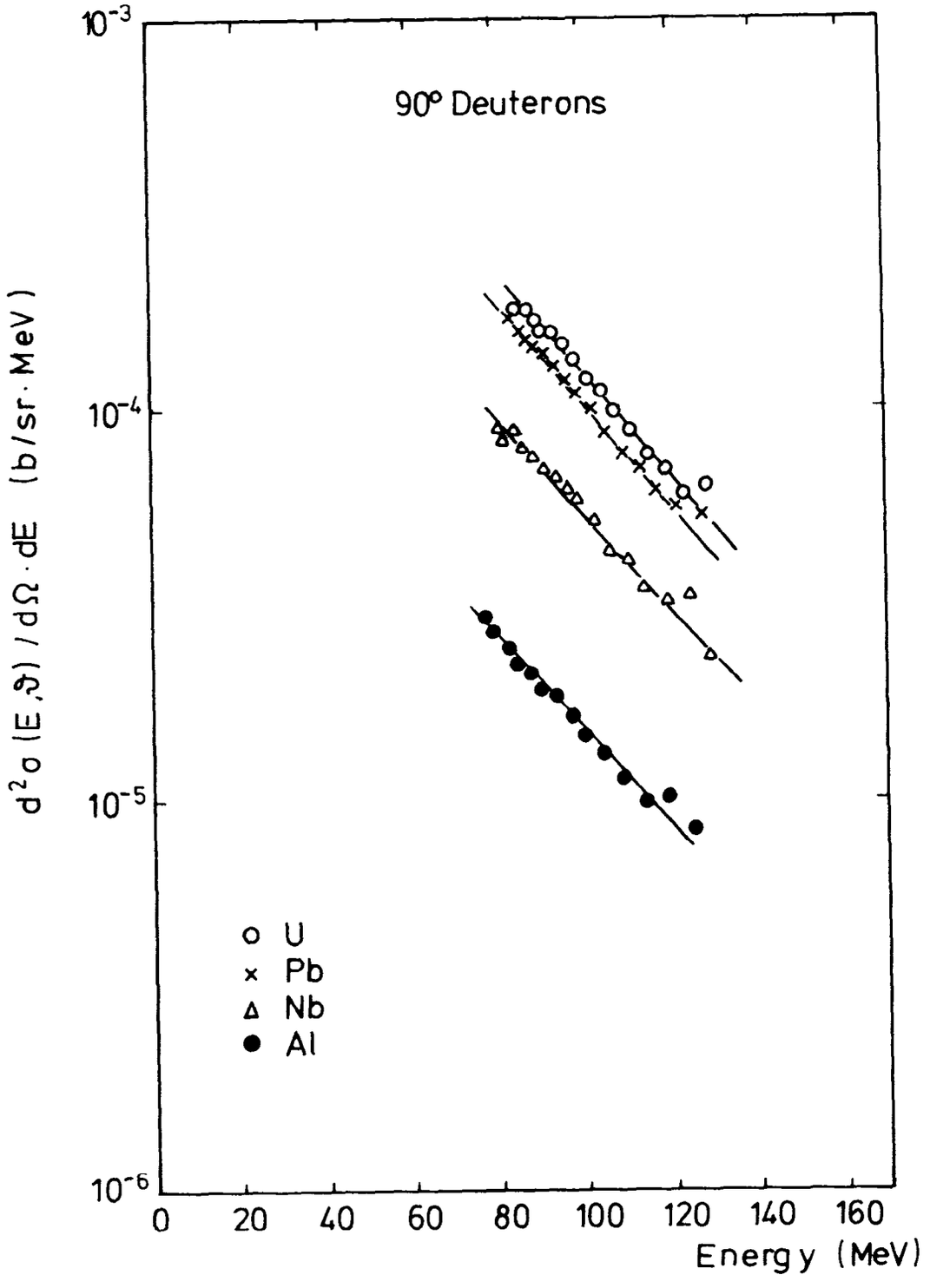

Figure 4 - Differential cross sections for deuterons emitted from aluminum, niobium, lead, and uranium at a laboratory angle of 90°. The character size indicates the statistical uncertainty.

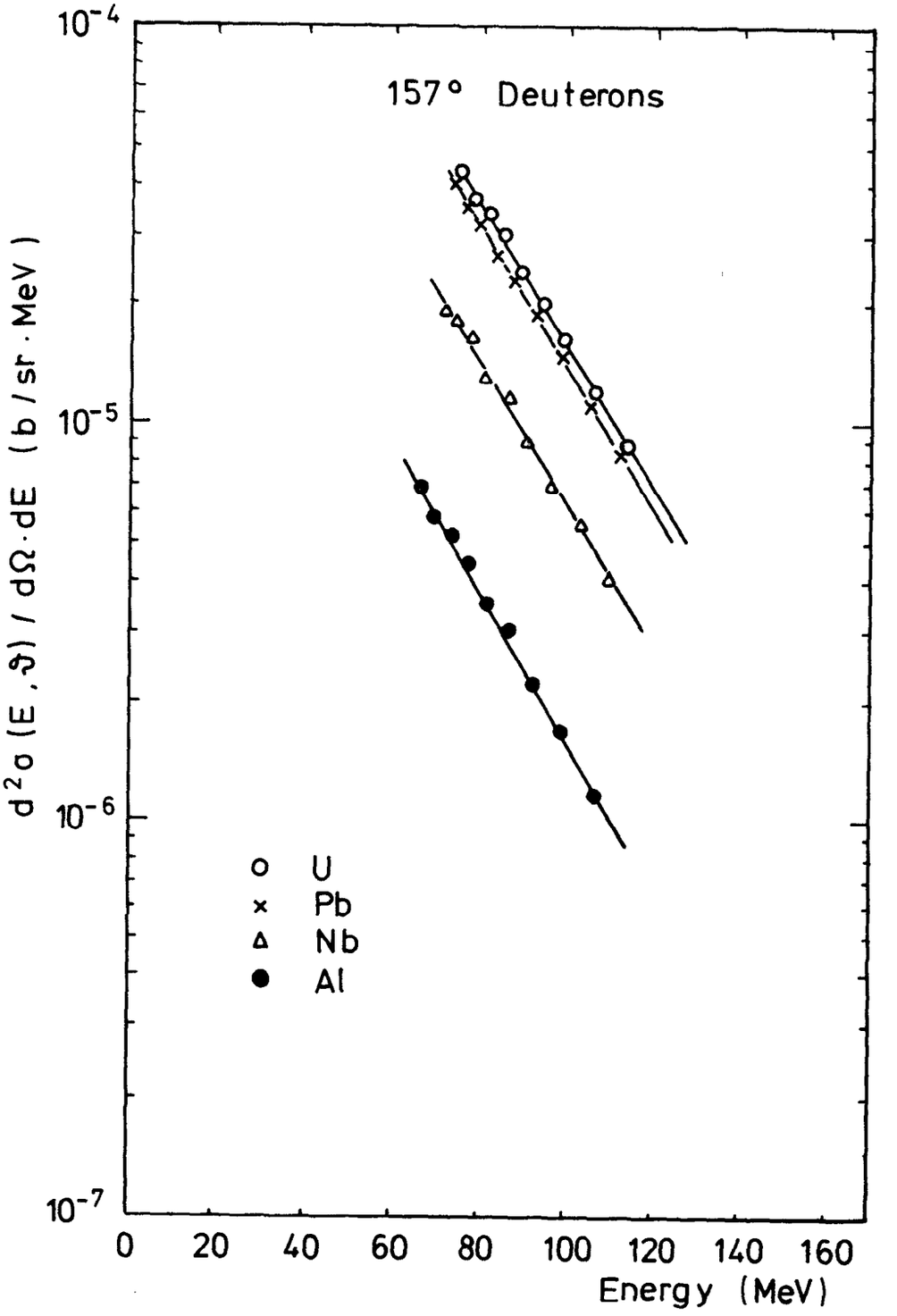

Figure 5 - Same as Fig. 4 except for a laboratory angle of 157°.

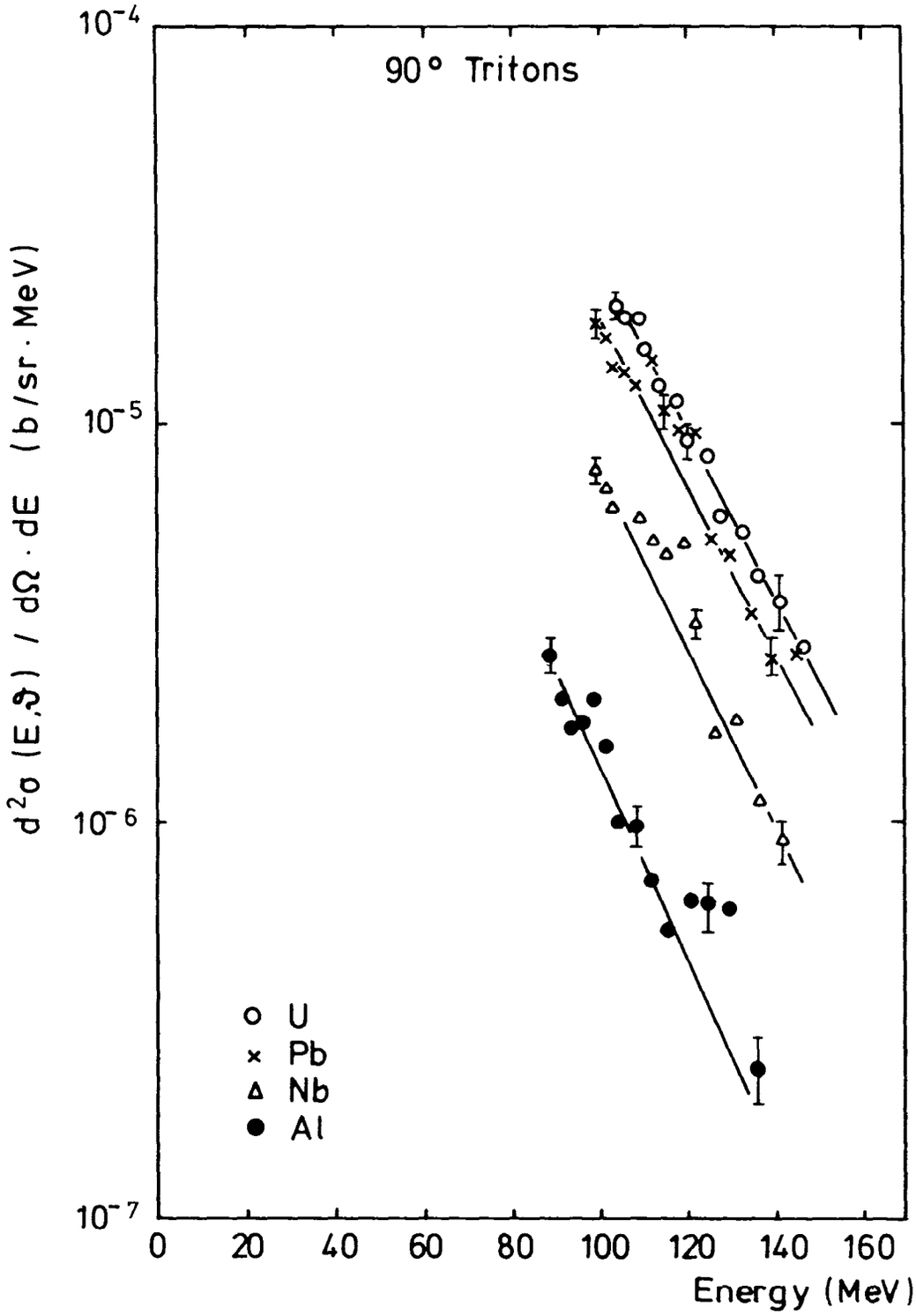

Figure 6 - Differential cross sections for tritons emitted from aluminum, niobium, lead, and uranium at a laboratory angle of 90°.

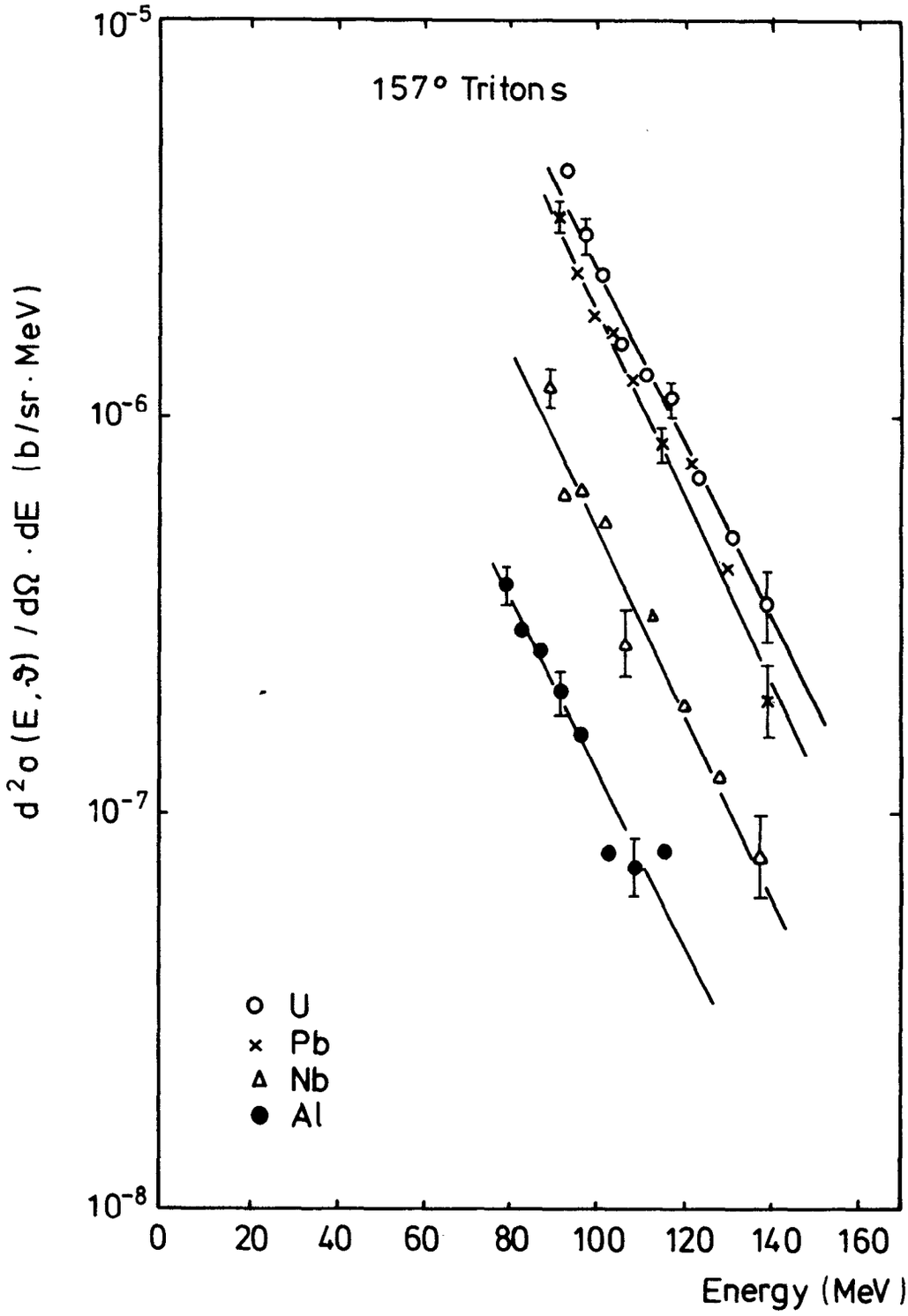

Figure 7 - Same as Fig. 6 except for a laboratory angle of 157°.

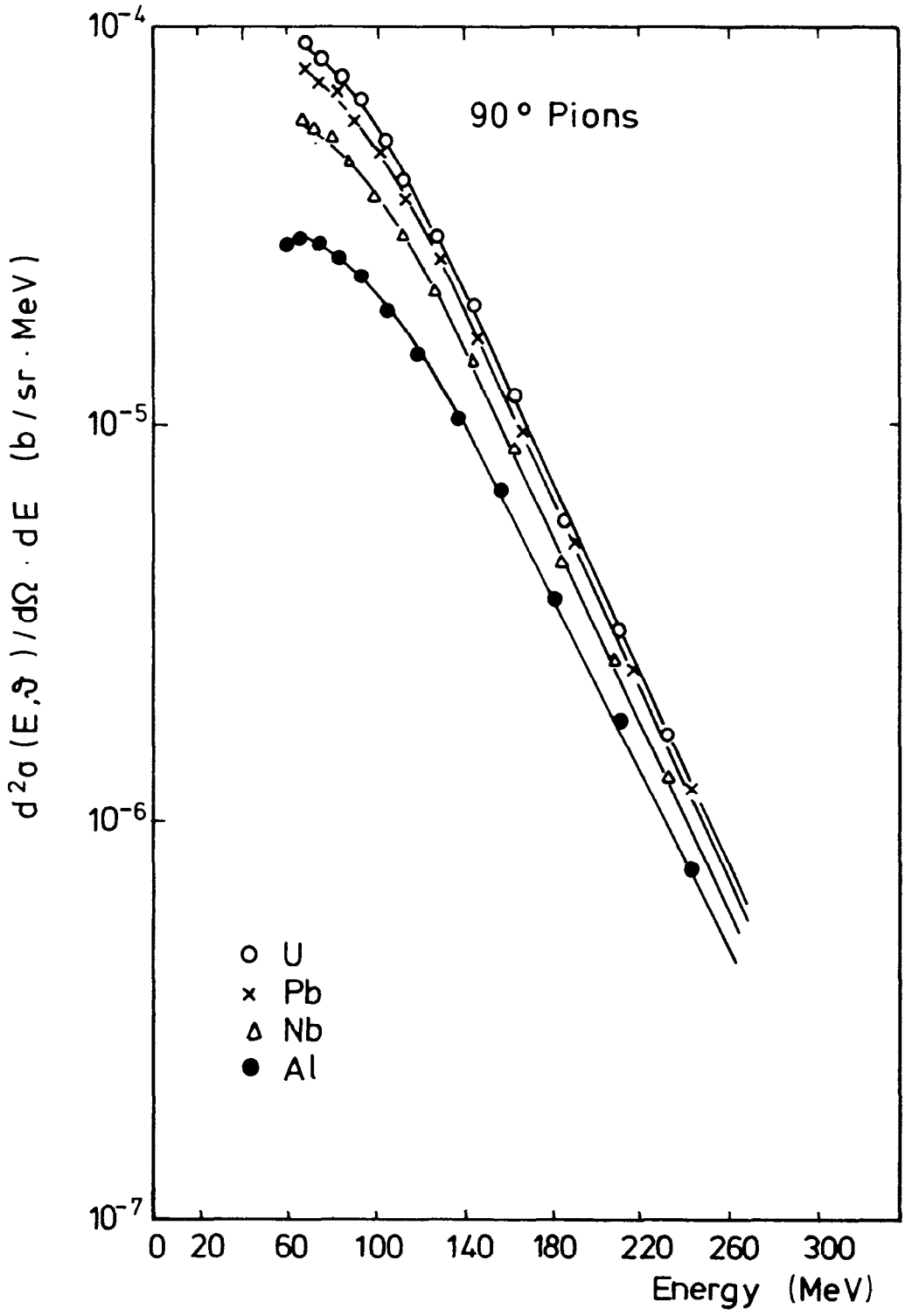

Figure 8 - Differential cross sections for pions (π^+ and π^-) emitted from aluminum, niobium, lead, and uranium at a laboratory angle of 90^o. The character size indicates the statistical uncertainty.

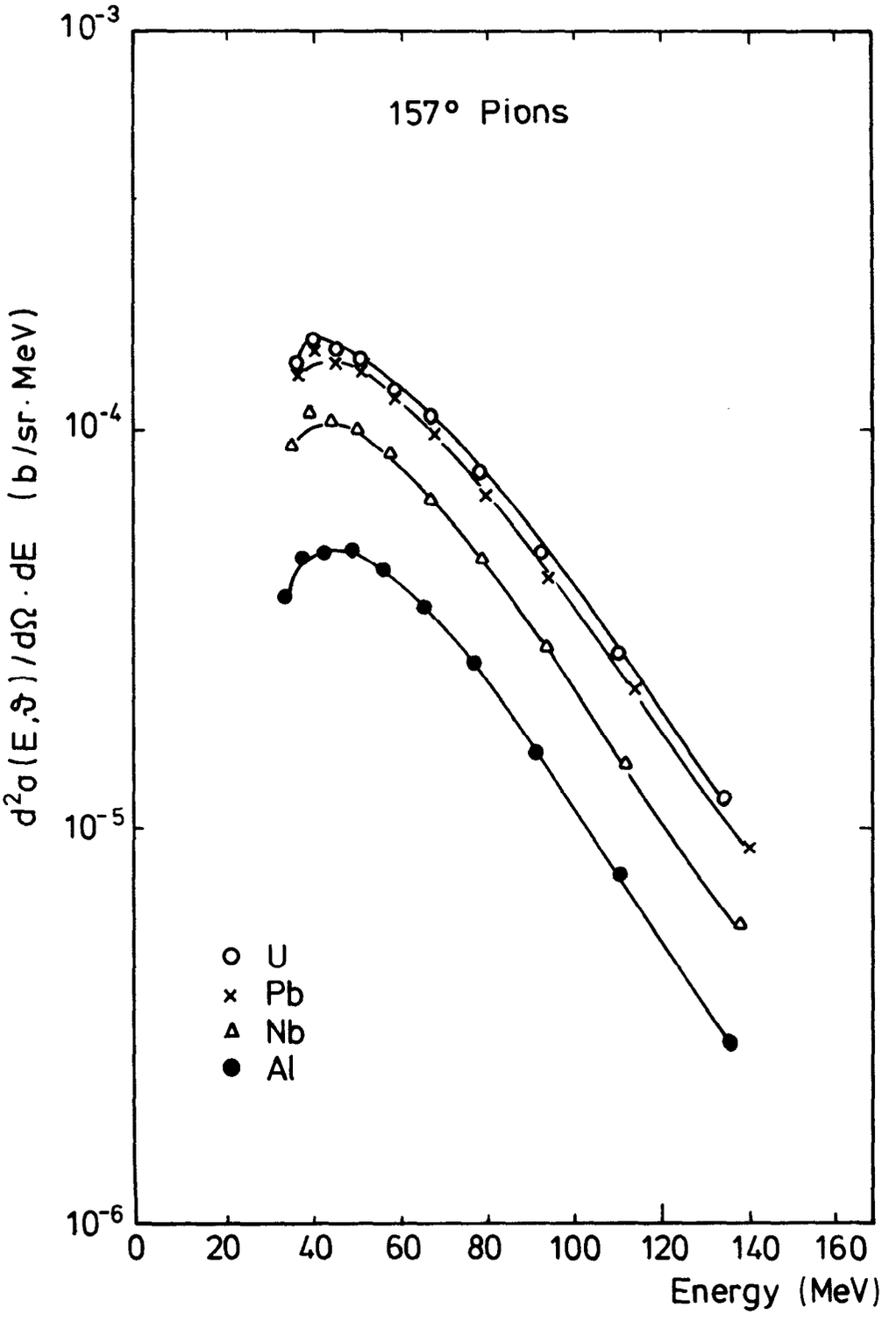

Figure 9 - Same as Fig. 8 except for a laboratory angle of 157°.

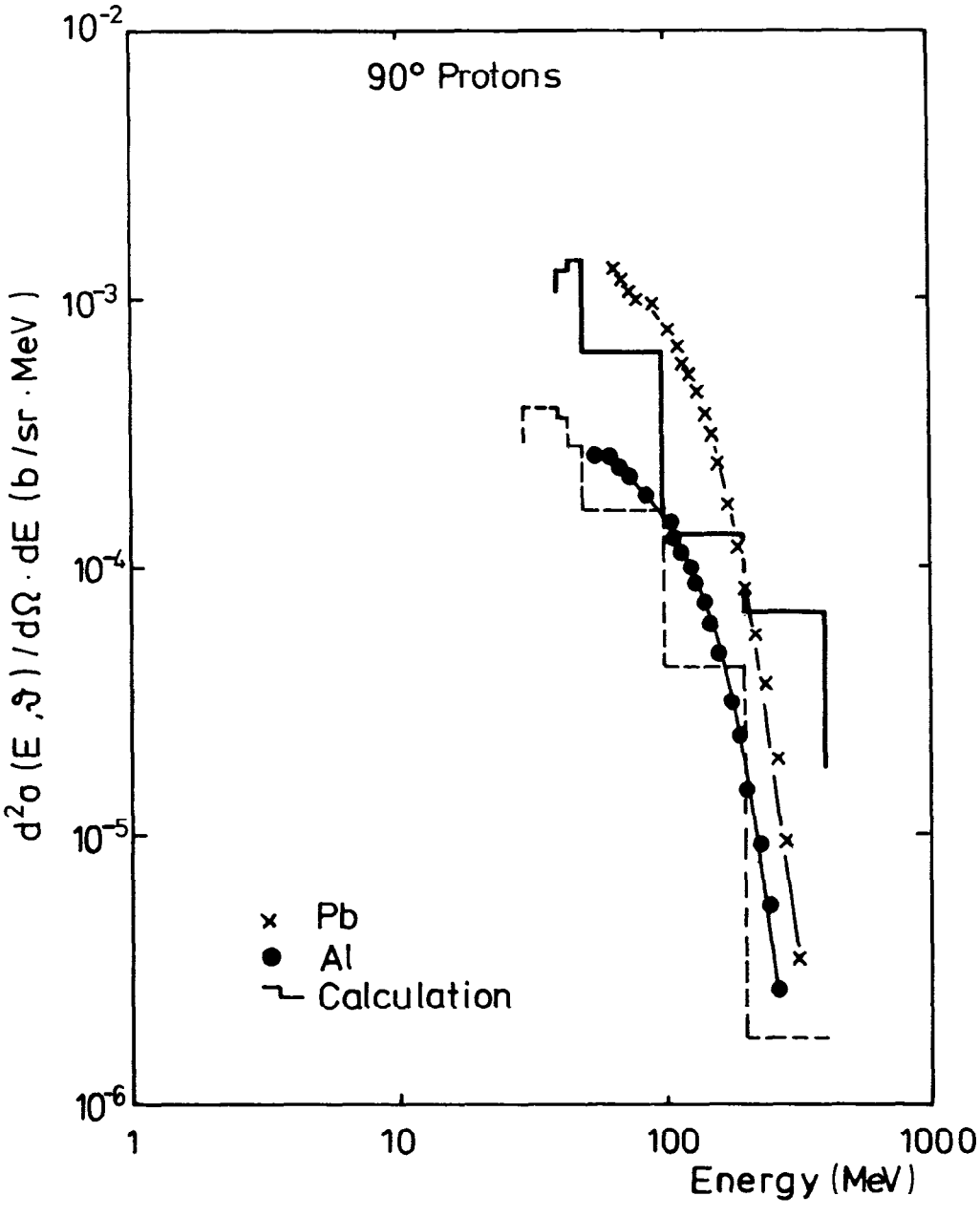

Figure 10 - Comparison of measured and calculated differential cross sections for secondary protons emitted from aluminum and lead at a laboratory angle of 90°.

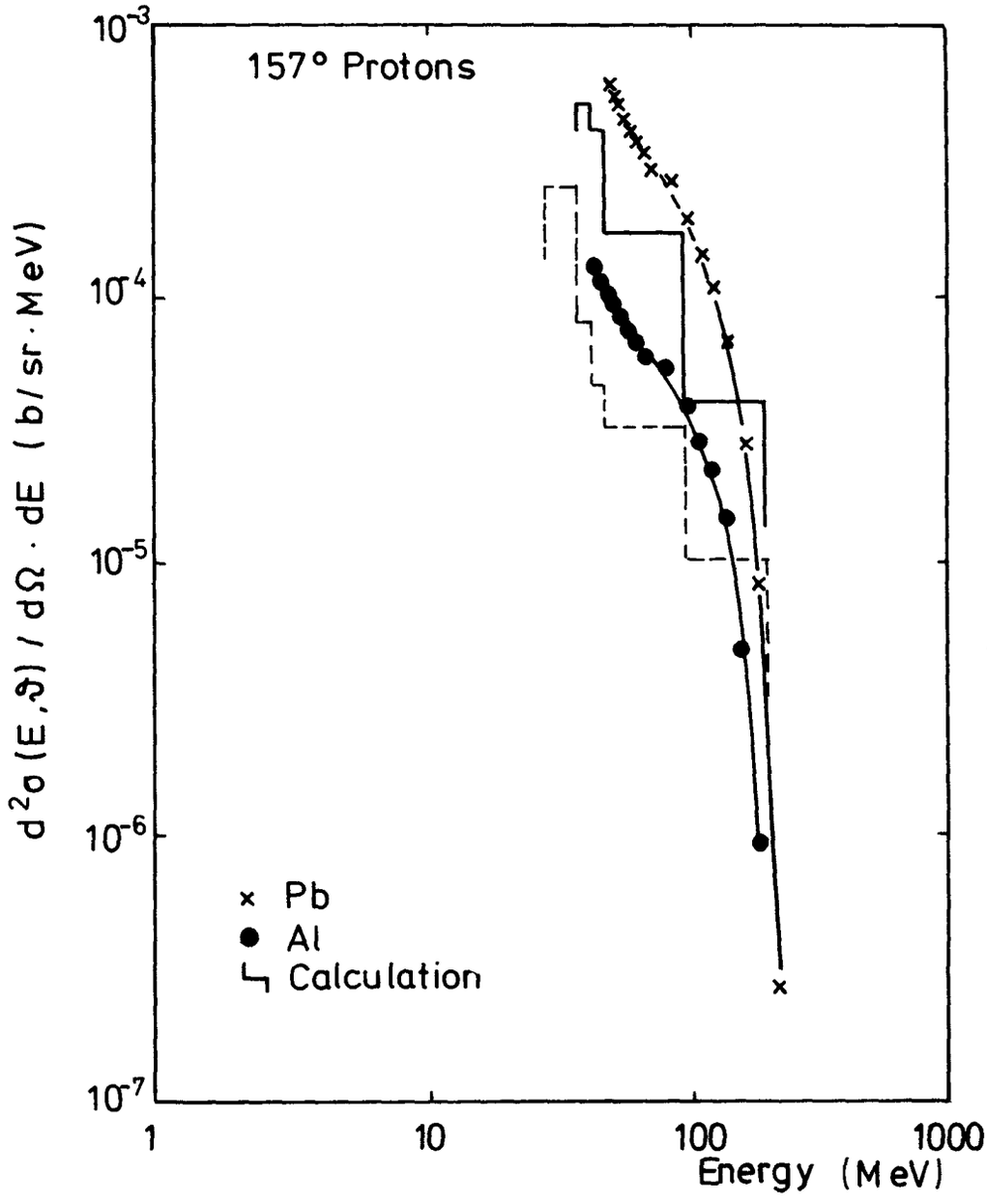

Figure 11 - Same as Fig. 10 except for a laboratory angle of 157°.

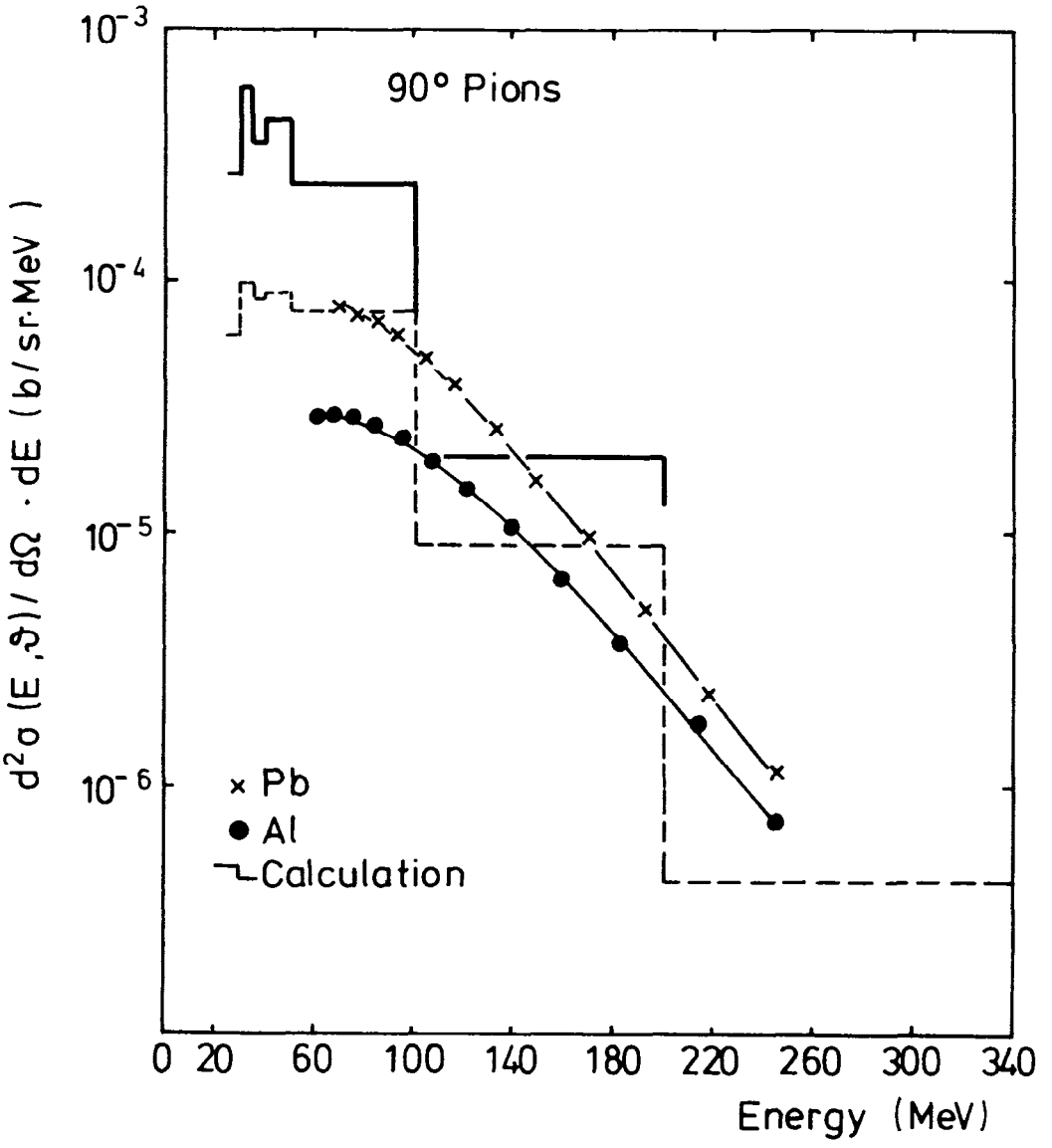

Figure 12 - Comparison of measured and calculated differential cross sections for pions (π^+ and π^-) emitted from aluminum and lead at a laboratory angle of 90°.

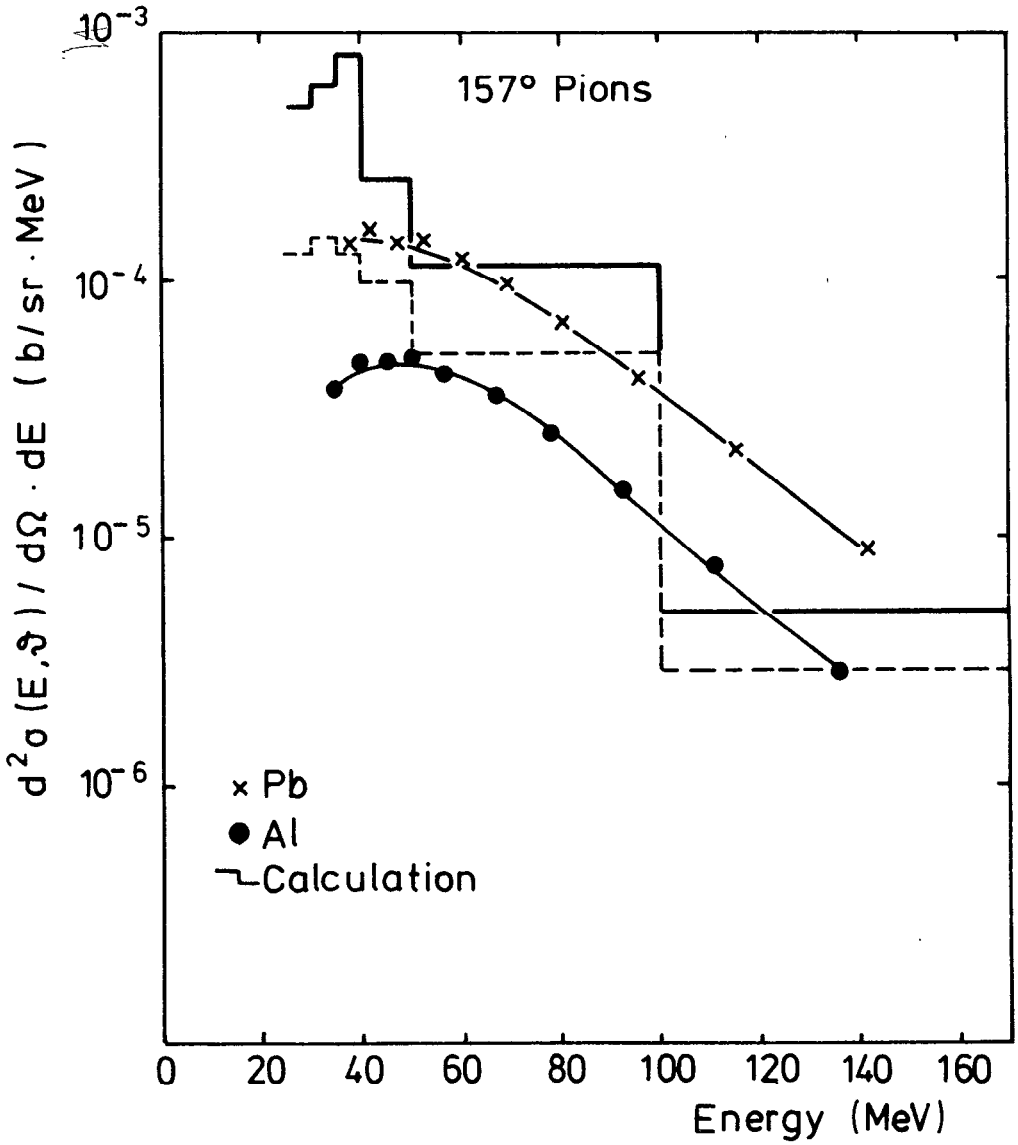

Figure 13 - Same as Fig. 12 except for a laboratory angle of 157°.